Bioorganic & Medicinal Chemistry 20 (2012) 3873–3879

Contents lists available at SciVerse ScienceDirect

Bioorganic & Medicinal Chemistry

journal homepage: www.elsevier.com/locate/bmc

Targeting of polyplex to human hepatic cells by bio-nanocapsules, hepatitis B virus surface antigen L protein particles

Masaharu Somiya [a], Nobuo Yoshimoto [a], Masumi Iijima [a], Tomoaki Niimi [a], Takehisa Dewa [b], Joohee Jung [c,d], Shun'ichi Kuroda [a,*]

[a] Department of Bioengineering Sciences, Graduate School of Bioagricultural Sciences, Nagoya University, Furo-cho, Chikusa, Nagoya 464-8601, Japan
[b] Graduate School of Engineering, Nagoya Institute of Technology, Nagoya 466-8555, Japan
[c] College of Pharmacy, Duksung Women's University, Seoul 132-714, South Korea
[d] Institute for Innovative Cancer Research, ASAN Medical Center, Seoul 138-736, South Korea

ARTICLE INFO

Article history:
Received 9 February 2012
Revised 15 April 2012
Accepted 16 April 2012
Available online 21 April 2012

Keywords:
Bio-nanocapsule
Gene delivery system carrier
Human hepatic cells
Hepatitis B virus surface antigen L protein particles
Polyethyleneimine

ABSTRACT

We have previously demonstrated that lipoplex, a complex of cationic liposomes and DNA, could be targeted to human hepatic cells in vitro and in vivo by conjugation with bio-nanocapsules (BNCs) comprising hepatitis B virus (HBV) surface antigen L protein particles. Because the BNC-lipoplex complexes were endowed with the human hepatic cell-specific infection machinery from HBV, the complexes showed excellent specific transfection efficiency in human hepatic cells. In this study, we have found that polyplex (a complex of polyethyleneimine (PEI) and DNA) could form stable complexes with BNCs spontaneously. The diameter and ζ-potential of BNC-polyplex complexes are about 240 nm and +3.54 mV, respectively, which make them more suitable for in vivo use than polyplex alone. BNC-polyplex complexes with an N/P ratio (the molar ratio of the amine group of PEI to the phosphate group of DNA) of 40 showed excellent transfection efficiency in human hepatic cells. When acidification of endosomes was inhibited by bafilomycin A1, the complexes showed higher transfection efficiency than polyplex itself, strongly suggesting that the complexes escaped from endosomes by both fusogenic activity of BNCs and proton sponge activity of polyplex. Furthermore, the cytotoxicity is comparable to that of polyplex of the same N/P value. Thus, BNC-polyplex complexes would be a promising gene delivery carrier for human liver-specific gene therapy.

© 2012 Elsevier Ltd. All rights reserved.

1. Introduction

Gene therapy is a promising therapeutic procedure for the treatment of intractable diseases. While selection of the most effective therapeutic gene is important, the gene delivery system (GDS) carrier delivering genes specifically to the affected parts in patient is also crucial to the success of gene therapy.[1] Currently, certain viruses (e.g., retrovirus, adenovirus, adeno-associated virus) are widely used as GDS carriers because of their remarkable ability to infect cells. However, viral carriers sometimes disturb the function of patient's chromosome by inserting their genomes into them, and viral components often elicit unexpected immunological reactions in patients.[2] These situations have led us to develop non-viral carriers that circumvent the potential virus-related problems.

Two major non-viral carriers, cationic liposomes (LPs) and cationic polymers, have been shown to form cationic complexes with nucleic acids, known as lipoplex (LPX) and polyplex (PPX), respectively. These complexes interact with the cell surface electrostatically, enter the cells by endocytosis, and the nucleic acids then translocate from the endosomes to the cytoplasm via the endosomal escape route. These carriers are safe in comparison with viral carriers, but their transfection efficiency is less efficient than viral carriers.[3] It has therefore been demonstrated that the transfection efficiencies of LPX can be enhanced by conjugation with viral envelope proteins (e.g., sendai virus,[4] influenza virus[5]), to create complexes known as virosomes. However, none of these GDS carriers, including viral carriers, have yet been able to accomplish pinpoint gene delivery in vivo.

Hepatitis B virus (HBV) specifically infects human hepatic cells, and the surface antigen (HBsAg) L protein plays a pivotal role in the early infection mechanism of HBV. The L protein can be overexpressed as hollow particles of about 100 nm in yeast cells.[6] Various materials incorporated into the L particles by electroporation can then be delivered specifically to human hepatic cells and tissues

Abbreviations: AFM, atomic force microscopy; BNC, bio-nanocapsule; GDS, gene delivery systems; HBV, hepatitis B virus; LPX, lipoplex; PEI, polyethyleneimine; PPX, polyplex; QCM, quartz crystal microbalance.

* Corresponding author. Tel./fax: +81 52 789 5227.
E-mail address: skuroda@agr.nagoya-u.ac.jp (S. Kuroda).

0968-0896/$ - see front matter © 2012 Elsevier Ltd. All rights reserved.
http://dx.doi.org/10.1016/j.bmc.2012.04.031

in vitro and in vivo.[7] Recently, it was revealed that the cell attachment and entry of L particles are mediated by the early infection mechanism of HBV.[8] The pre-S1 region in the N-terminal half of the L protein was shown to possess membrane fusogenic activity (unpublished data), which may play a crucial role in the translocation of HBV (as well as L particles) from endosomes to the cytoplasm. We therefore designated this useful GDS carrier as bio-nanocapsule (BNC). The materials required for viral replication have been removed from BNC to enable its use as an immunogen for HB vaccine over the last three decades. BNC is therefore a proven safe material. Furthermore, BNC can be retargeted to various cells and tissues by substituting bio-recognition molecules (e.g., antibodies,[9] lectins,[10] cytokines[7]) for the human hepatic cell-receptor located in the pre-S1 region. We previously observed that BNC could form a stable complex with LPX, and the BNC-LPX complex could be used for pinpoint in vitro and in vivo gene delivery.[11] The BNC-LPX fusion allowed us to obtain a substantial amount of BNC-based GDS carrier efficiently and reproducibly. Thus, BNC is a promising biomaterial for endowing non-viral carriers with excellent transfection efficiency and high specificity for human hepatic cells.

In this study, we aimed to apply the BNC conjugation technique to polyethyleneimine (PEI), one of the major cationic polymers used for GDS. The PEI-derived PPX induces the rupture of endosomes by the accumulation of protons from the cytoplasm (proton sponge effect[12]), and thus enhances endosomal escape of nucleic acids. The conjugation with BNC was expected to confer both human liver specificity and membrane fusogenic activity to PPX. In this report, we demonstrate that PPX spontaneously forms stable complexes with BNCs, and that these BNC–PPX complexes enable more efficient and specific transfection of hepatic cells than PPX alone.

2. Materials and methods

2.1. Bio-nanocapsule (BNC)

BNC was prepared from *Saccharomyces cerevisiae* AH22R$^-$ strain harboring BNC-expression plasmid pGLDLIIP39-RcT.[6] BNC was purified as described previously.[13]

2.2. Cells

The human hepatocellular carcinoma cell line, HuH-7, and the human lung adenocarcinoma cell line, A549, were obtained from RIKEN (Wako, Japan) and cultured in Dulbecco's modified Eagle's medium (DMEM, Nacalai Tesque, Kyoto, Japan) supplemented with 10% (v/v) fetal bovine serum (FBS, PAA Laboratories GmbH, Linz, Austria) at 37 °C in a 5% CO_2 humidified atmosphere.

2.3. QCM (quartz crystal microbalance) analysis

The interaction of BNCs with PEI was measured using a QCM model Twin-Q (As One, Osaka, Japan). The sensor chip of the QCM consisted of a 9 mm-diameter disk made from an AT-cut 27 MHz quartz crystal with gold electrodes on both sides (diameter, 2.5 mm; area, 4.9 mm^2). A frequency change (ΔF) of 1 Hz corresponded to a weight change of 6 pg/mm^2. The temperature of the measuring bath (500 μl) was kept at 25 °C, and the bath was mixed at 600 rpm with a stirring tube. Measurements were taken until a stable frequency (less than 4 Hz) was observed for >2 min.

2.4. Preparation of BNC–PPX complexes

BNC–PPX complexes were prepared by incubating BNCs with branched 25 kDa PEI (polyethyleneimine; Sigma, St. Louis, MO) in phosphate-buffered saline (PBS; 137 mM NaCl, 10 mM Na_2PO_4 and 2 mM KH_2PO_4, pH 7.4) at room temperature for 20 min, followed by incubation with the pCAG-Luc3 luciferase expression plasmid (kindly provided by Professor Naoto Oku at University of Shizuoka) at room temperature for 20 min. Protein concentrations were determined using the BCA Protein Assay Kit (Pierce, Rockford, IL) with BSA (bovine serum albumin, Wako, Osaka, Japan) as the standard.

2.5. AFM (atomic force microscopy) analysis

Sample solutions were spotted onto the mica chip, briefly dried in air, and analyzed on an AFM model SPA-400 (SII NanoTechnology Inc., Chiba, Japan). Images were acquired at the 500 × 500 nm scale at room temperature in air.

2.6. Diameters and ζ-potentials

The diameters (*Z*-averages) and ζ-potentials of the samples were measured at 25 °C in water using a Zetasizer Nano ZS (Malvern Instruments, Worcestershire, UK).

2.7. Luciferase assay

Cells (about 5 × 10^4 cells/well) were grown in a 24-well cell culture plate for one day, and then incubated with freshly prepared PPX alone or BNC–PPX complexes in serum-free medium. In case of competition assay, cells were pre-incubated with BNCs at 126 ng/ml (as protein) for 30 min before each complex was added. The medium was changed to FBS-containing medium after 6 h. After 42 h, the cells were washed twice with PBS, then lysed with 100 μl of Passive Lysis Buffer (Promega, Madison, WI). Ten microliter of cell lysate was mixed with 50 μl of Steady Glo luciferase substrate solution (Promega), and analyzed on a microplate reader Synergy2 (Biotek, Winooski, VT). Relative luminescence units (RLU) for each sample were defined as the luminescence value divided by the protein concentration.

2.8. Analysis of endosomal escape

HuH-7 cells (about 5 × 10^4 cells/well) were pretreated with 1 or 10 nM bafilomycin A1, a selective vacuolar proton pump inhibitor (Wako), for 30 min, and subjected to luciferase assay. To visualize the intracellular localization of PPX and BNC–PPX complexes, HuH-7 cells (about 1.5 × 10^4 cells) grown in a 8-well glass-bottomed chamber (Thermo Fisher Scientific, Waltham, MA, USA) were treated with 100 nM bafilomycin A1 for 30 min, contacted with PPX or BNC–PPX complexes (N/P = 40, 800 ng/ml pCAG-Luc3, 500 ng/ml (as protein) BNC), of which the PEI moiety was labeled with FITC (Pierce) , and 200 μg/ml Texas Red-labeled dextran (endosome marker, 70,000 MW, neutral; Invitrogen, Carlsbad, CA, USA). After 30 min, cells were washed with DMEM, and cultured for 2 h in the presence of bafilomycin A1. The cells were washed with acid buffer (200 mM acetic acid, 500 mM NaCl (pH 2.5)) for 5 min to remove excess fluorescence from cell surface, washed with PBS, and then fixed in 4% (w/v) PFA in PBS at room temperature for 20 min. Concurrently, nuclei were stained with Hoechst 33342 (Invitrogen) in PBS at room temperature for 20 min. The fluorescence was observed under an FV-1000D confocal laser scanning microscope (Olympus, Tokyo, Japan). The areas of fluorescent dots derived from PPX or BNC–PPX complexes in HuH-7 cells were measured by using a software FV-10-ASW (Olympus).

2.9. Cytotoxicity assay

HuH-7 (target cells) and A549 (non-target cells) were seeded in 96-well cell culture plates at about 5 × 10^3 cells/well, cultured for

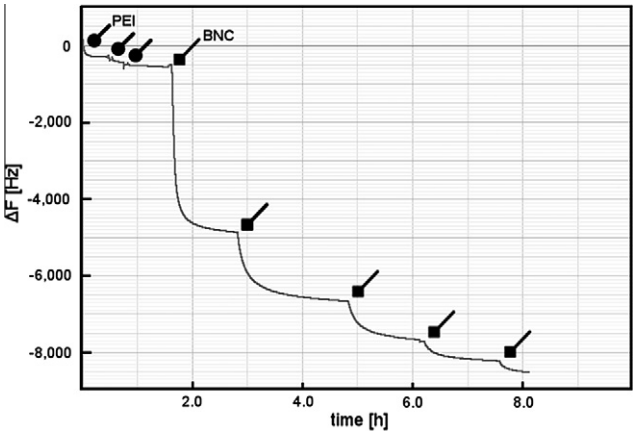

Figure 1. Complex formation of PEI with BNC. PEI (2 μg/injection) was applied into a QCM sensor bath three times (closed circles). After washing with PBS, BNCs (5 μg/injection) were applied into the sensor bath five times (closed triangles).

24 h, and then incubated with PPX alone or BNC–PPX complexes at different N/P ratios (10, 40, and 80) and plasmid concentrations (10, 100, 200, and 500 ng/ml). Forty-eight hours after the addition of the BNC–PPX complexes, WST-8 assay was performed using a commercial WST-8 assay reagent (Nacalai Tesque) according to the manufacturer's protocol. The formation of tetrazolium from WST-8 was monitored on a microplate reader at 450 nm.

3. Results and discussion

3.1. Complex formation of PEI with BNCs

PEI was adsorbed onto the sensor chip of QCM to saturation. As shown in Figure 1 and 16.05 ± 5.17 ng (n = 3, mean ± SD) of PEI (corresponding to −545.9 ± 175.9 Hz (n = 3, mean ± SD) of ΔF) could be fixed onto the chip. Next, BNCs were added to the sensor bath of a QCM to determine the amount of BNCs that could bind to PEI. We determined that 195.4 ± 39.7 ng (n = 3, mean ± SD) of BNCs (corresponding to −6646 ± 135.0 Hz (n = 3, mean ± SD) of ΔF) interacted with PEI. As control, BNCs were also adsorbed onto the chip at 88.4 ± 17.1 ng (n = 3, mean ± SD), corresponding to −3007 ± 581.6 Hz (n = 3, mean ± SD) of ΔF. Accordingly, 1 ng of PEI was estimated to bind to at least 107.0 ± 39.7 ng (n = 3, mean ± SD) of BNCs, presumably by electrostatic interaction due to its negatively charged surface (ζ-potential of BNCs, −15.6 mV).

3.2. Physicochemical properties of BNC–PPX complexes

AFM observation in air indicated that PPX of N/P = 40 (N/P, the molar ratio of the amine group of PEI to the phosphate group of DNA), BNCs, and BNC–PPX complexes (N/P = 40) have dome-shaped structures with distinct heights (Fig. 2). PPX was 3.85 ± 0.73 nm in height (n = 10, mean ± SD) and 146.1 ± 15.5 nm in diameter (n = 88, mean ± SD) (panel A), BNC was 7.94 nm in height (n = 10, mean ± SD) and 49.9 ± 21.5 nm in diameter (n = 19, mean ± SD) (panel B), and BNC–PPX complexes were 62.2 ± 8.32 nm in height (n = 10, mean ± SD) and 169.2 ± 18.7 nm in diameter (n = 29, mean ± SD) (panel C). DLS (dynamic light scattering) analysis revealed that the Z-averages of PPX (N/P = 40), BNCs, and BNC–PPX complexes (N/P = 40) were 187 nm (PDI = 0.125), 74.0 nm (PDI (poly-diversity index) = 0.173), and 241 nm (PDI = 0.154), respectively. The volumes of these particles calculated by DLS agreed well with those of the dome-shaped structures observed by AFM, suggesting that these materials were not ruptured on the mica chip of AFM even in air.

At increasing N/P ratios, the diameters (Z-averages) of PPX were dramatically decreased from about 1 μm to about 200 nm, whereas the diameters of BNC–PPX complexes did not change greatly (Fig. 3A). The ζ-potentials of PPX and BNC–PPX complexes were kept at about 30 and 5 mV at an N/P ratio of more than five (Fig. 3B). For systemic administration, it is important for nanocarriers to escape from the capture by the reticuloendothelial system in the body. Thus, the use of nanocarriers of 100–200 nm in diameter is strongly recommended.[14] As for the surface charge, positively charged materials tend to bind electrostatically to various components in blood (e.g., plasma proteins, vessel endothelia, and erythrocytes[15]), leading to rapid clearance from the body. Due to its large size and positive charge, PPX has so far been deemed inadequate for in vivo use. Conjugation with BNC would prevent PPX from forming non-specific and unwanted interactions with blood components, and also improve the pharmacokinetics of PPX for in vivo use.

3.3. Transfection efficiency and cell specificity of BNC–PPX complexes

BNC–PPX complexes were prepared by mixing BNCs with different amounts of PEI, followed by mixing with the mammalian luciferase expression vector to formulate various N/P ratios (10, 20, and 40) (see section 2.4). Each complex was added to the medium of HuH-7 cells (the target cells for BNC) and A549 cells (the non-target cells for BNC) in serum-free medium for 6 h. PPX prepared at the same N/P ratios was used as the control. After incubation in FBS-containing medium for 42 h, the cell lysate of each well was subjected to luciferase assay (Fig. 4A and B). BNC–PPX complexes of higher N/P ratio showed high transfection efficiency in HuH-7 cells (closed bars in Fig. 4A), while the transfection efficiency of PPX was low and independent of N/P ratio (open bars in Fig. 4A). In non-target A549 cells, both BNC–PPX complexes and PPX showed low transfection efficiency (Fig. 4B). In particular, BNC–PPX complexes

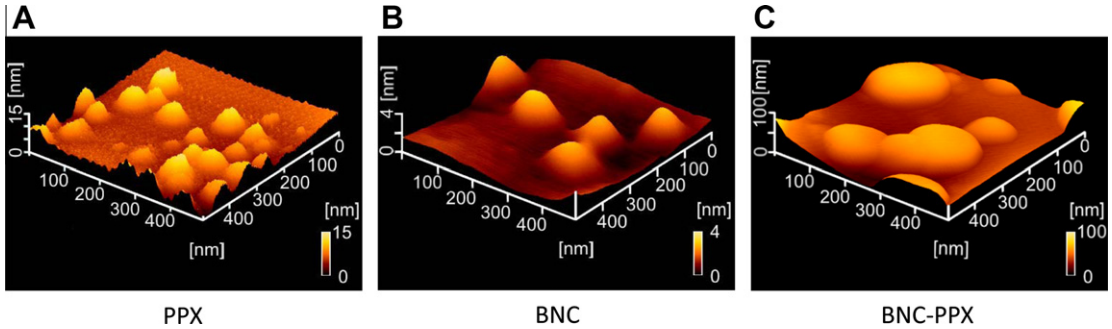

Figure 2. AFM analyzes of PPX, BNC and BNC–PPX complexes. (A) PPX of N/P = 40, (B) BNC, and (C) BNC–PPX complexes of N/P = 40 were observed under AFM. Samples were adsorbed onto a mica chip, dried, and then scanned in DFM (dynamic force microscopy) mode. Color bars indicate the heights of the complexes.

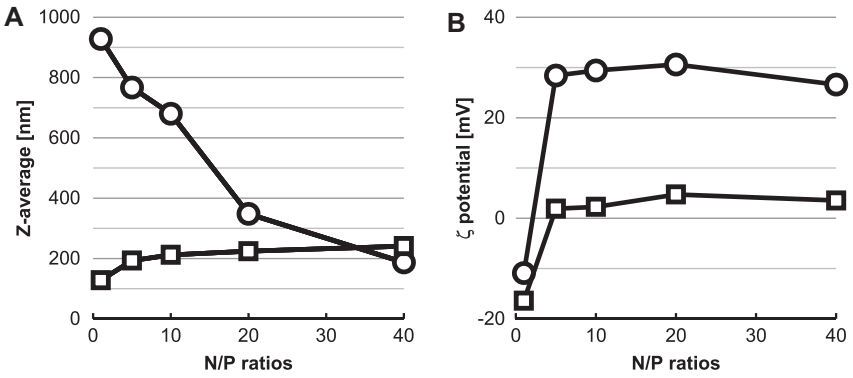

Figure 3. Diameters and surface charges of BNC–PPX complexes and PPX alone. *Z*-averages (A) and ζ-potentials (B) of BNC–PPX complexes (open squares) and PPX (open circles) were measured using a Zetasizer Nano ZS.

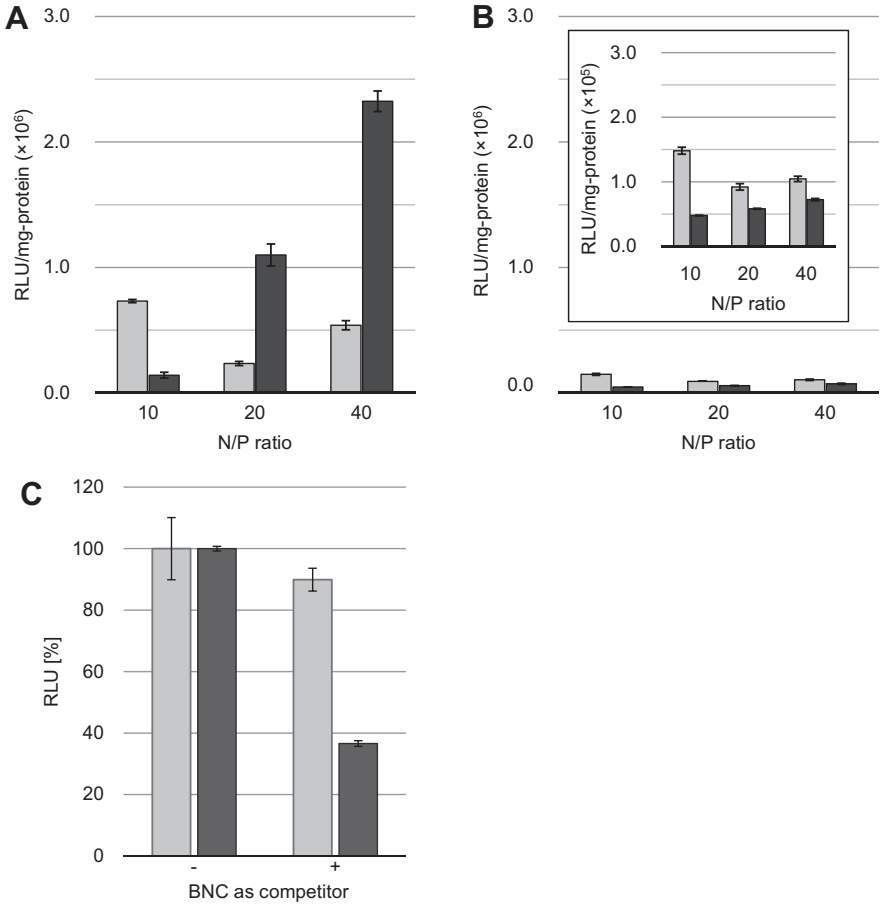

Figure 4. In vitro transfection efficiency of BNC–PPX complexes. (A) Human hepatocellular carcinoma HuH-7 cells and (B) lung adenocarcinoma A549 cells. Cells were transfected with PPX (open bars) or BNC–PPXBNC–PPX complexes (closed bars) of different N/P ratios (10, 20, and 40). (C) Competition assay using BNC as competitor. After incubating with BNC at 126 ng/ml (as protein), HuH-7 cells were transfected with PPX (open bars) or BNC–PPX complexes (closed bars). For all panels, the amounts of plasmid DNA and BNCs were 200 ng/ml and 126 ng/ml (as protein), respectively. Luciferase activity (RLU, relative luminescence units) was measured 48 h after transfection ($n = 4$, means ± SEM).

of N/P = 40 showed about 4.5-fold higher transfection efficiency than PPX alone in HuH-7 cells (Fig. 4A), which was not enhanced even at N/P = 80 (data not shown). Although the ζ-potentials of BNC–PPX complexes were constantly neutral at N/P ratios of 5 to 40 (see Fig. 3B), the transfection efficiency was elevated in an N/P ratio-dependent manner. As mentioned in Fig. 3, the amount of conjugated BNCs might be increased in an N/P ratio-dependent manner, resulting in keeping the size and surface charge of BNC–PPX complex at about 200 nm and neutral, respectively. The BNC moiety of BNC–PPX complexes might contribute to both specific binding and efficient uptake in human hepatic cells, both of which were recently shown in BNC itself by Yamada et al.[8]

Furthermore, to evaluate the effect of BNC on specific binding of BNC–PPX complexes to human hepatic cells, we added BNC to the luciferase assay using HuH-7 cells as competitor. Transfection efficiency of BNC–PPX complexes was reduced by the addition of BNC, whereas that of PPX was not affected (Fig. 4C). These results strongly suggested that BNC–PPX complexes, similar to BNC itself,[8]

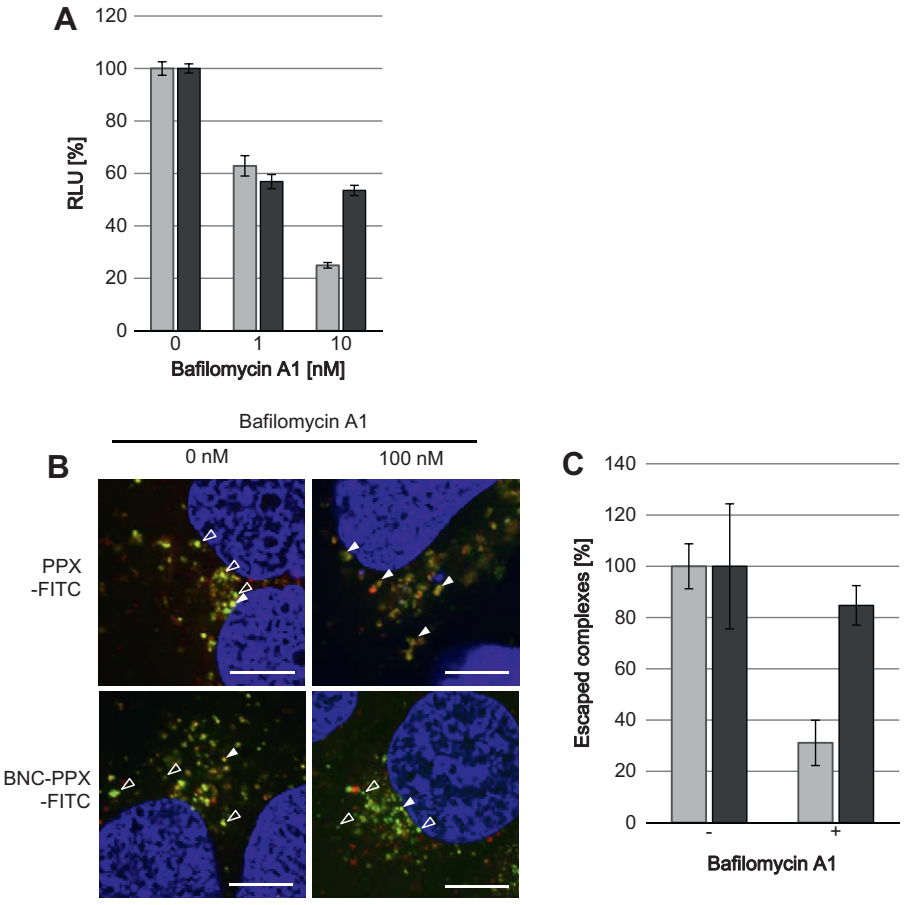

Figure 5. Inhibition of endosomal escape by bafilomycin A1. (A) Transfection efficiency in HuH-7 cells in the presence of bafilomycin A1. Cells were transfected with PPX (open bars) and BNC–PPX complexes (closed bars), of which the composition was described in Figure 4, cultured with bafilomycin A1 for 48 h, and subjected to luciferase assay (n = 6, means ± SEM). Luciferase activity (RLU, relative luminescence units) of non-treated cells was defined as 100%. (B) Intracellular localization of PPX and BNC–PPX complexes in HuH-7 cells. FITC-labeled PPX and BNC–PPX complexes (green dots), dextran-Texas Red (red dots), and Hoechst 33342 (blue). Closed and open triangles represent merged dots (yellow dots, colocalized with endosomes) and green dots (green dots, escaped complexes), respectively. Bars, 10 μm. (C) Efficiency of endosomal escape of PPX or BNC–PPX complexes. Areas of each fluorescent dot of Figure 5B were measured by a software FV-10-ASW. The ratio of (areas of green dots) to (areas of green and yellow dots) was defined as the efficiency of endosomal escape. The ratios in untreated HuH-7 cells were calibrated to 100% (n = 3, means ± SD).

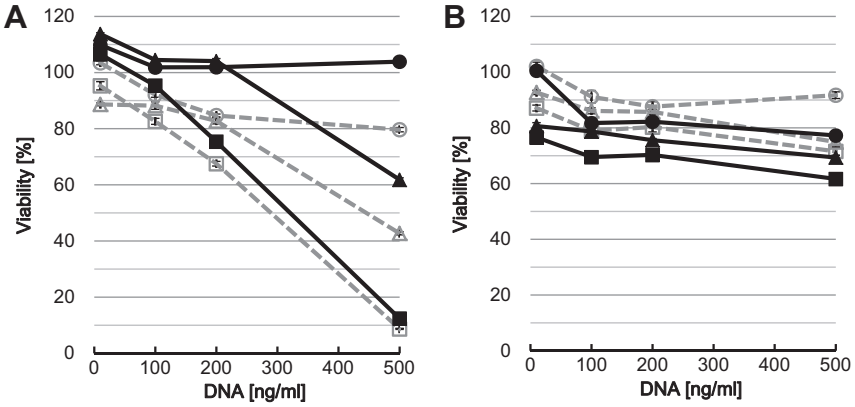

Figure 6. Cytotoxicity of BNC–PPX complexes and PPX. HuH-7 cells (A) and A549 cells (B) were treated with BNC–PPX complexes (solid lines, closed markers) and PPX (dashed lines, open markers), which were prepared at different N/P ratios of 10 (circles), 40 (triangles) and 80 (squares). After incubation for approximately 48 h, the cells were subjected to WST-8 assay (n = 6, means ± SEM).

specifically interacted with unidentified receptors for HBV on human hepatic cells and then entered into cells more efficiently than PPX. Therefore, as well as LPX,[11] PPX may be endowed with the HBV-derived infection machinery by conjugation with BNCs, facilitating the efficient delivery of PPX specifically to human hepatic cells.

3.4. Effect of BNC on endosomal escape of BNC–PPX complexes

To study the involvement of endosome acidification on endosomal escape of both PPX and BNC–PPX complexes, we added bafilomycin A1, a selective vacuolar proton pump inhibitor,[16] to luciferase assay using HuH-7cells. The transfection efficiency of

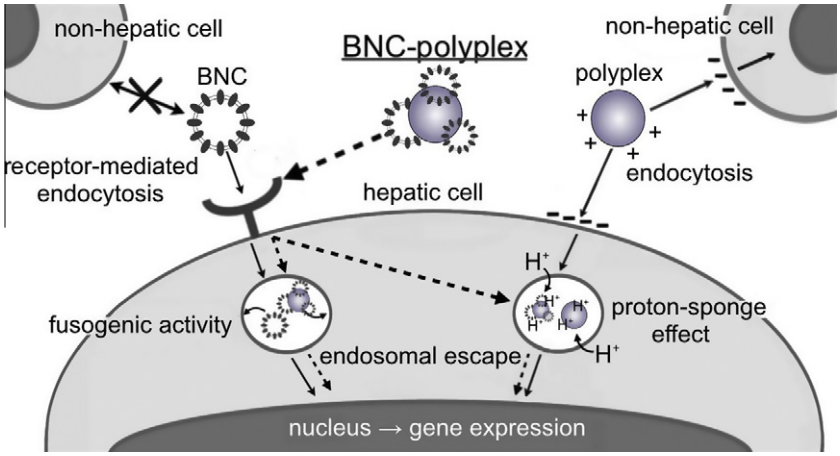

Figure 7. Working hypothesis for the cellular attachment and entry of BNC, BNC–PPX complexes, and PPX in human hepatic cells. According to the early infection mechanism of HBV, BNCs attach to postulated HBV receptor(s) specifically expressed on the surface of human hepatic cells, and subsequently enter into the cell via receptor-mediated endocytosis. In the late endosomes, BNCs fuse with endosomal membranes through their endogenous low pH-dependent membrane fusogenic peptide, followed by translocation from endosomes to the cytoplasm (endosomal escape). In contrast, PPX interacts with cell membranes electrostatically, and then enters into cells via non-specific endocytosis. In the late endosomes, PPX is thought to induce the disruption of endosomes by its proton-sponge activity, followed by endosomal escape. BNC–PPX complexes are expected to enter into cells in the same way as BNCs and exert endosomal escape synergistically by the membrane fusion activity of BNC and the proton sponge activity of PPX.

PPX was significantly decreased by bafilomycin A1 (open bars in Fig. 5A), presumably due to the inhibition of proton sponge effect crucial for endosomal escape of PPX.[16] Contrary, the transfection efficiency of BNC–PPX complexes was also decreased by bafilomycin A1, but the degree of inhibition was moderate as compared with PPX (closed bars in Fig. 5A). Furthermore, the intracellular trafficking of PPX and BNC–PPX complexes was investigated with FITC-labeled forms in HuH-7 cells. After the incubation without bafilomycin A1 for 2 h, large part of these complexes was found to escape from endosomes which was visualized with Texas Red-labeled dextran (Fig. 5B, left panels). While PPX was colocalized with endosomes (closed triangles) in the presence of 100 nM bafilomycin A1, BNC–PPX complexes still escaped from endosomes (open triangles). Based on the areas of fluorescent dots in Fig. 5B, when the endosomal escape of both complexes in the absence of bafilomycin A1 was defined as 100%, the treatment with bafilomycin A1 was found to decrease the endosomal escape of PPX and BNC–PPX complexes by 70% and 15%, respectively (Fig. 5C). Since BNC was reported to harbor low pH-dependent membrane fusogenic domains,[17,18] it was postulated that BNC–PPX complexes can escape from endosomes not only by proton sponge effect derived from PPX moiety but also by presumably membrane fusogenic activity derived from BNC moiety.

3.5. Cytotoxicity of BNC–PPX complexes

HuH-7 cells (the target cells for BNC) and A549 cells (the non-target cells for BNC) were incubated with BNC–PPX complexes containing 10–500 ng/ml of DNA, cultured for 48 h, and then subjected to WST-8 assay. BNC–PPX complexes showed slightly less cytotoxicity than PPX in HuH-7 cells (Fig. 6A), and comparable cytotoxicity in A549 cells (Fig. 6B). Because the viability curves of BNC–PPX complexes coincided with those of PPX, the cytotoxicity of BNC–PPX complexes might be attributed to the cationic polymer, in which the excess positive charge mainly contributes to its cytotoxicity.[19] Minimizing the cytotoxicity of GDS carriers is an important issue for enabling gene therapy to be conducted safely. Some researchers attempted to reduce the cytotoxicity of the cationic polymer by either conjugation with various molecules (e.g., hyaluronic acid[20]) to neutralize the surface charge, or modification with functional groups (e.g., disulfide bond[21]) to improve biodegradability. By combination with these improved cationic polymers, the BNC–PPX complexes may become safer as GDS carriers.

3.6. Advantages of BNC–PPX complexes

PEI and other cationic polymers have been retargeted to tumors mainly by conjugation with various bio-recognition molecules, such as anti-HER2 antibody,[22] transferrin,[15] RGD peptide,[23] and hyaluronic acid.[24] These modified carriers appear to be favorable for in vivo pinpoint gene delivery; however, they often show lower transfection efficiency than the original cationic polymers. PEI was used to modify the tropism and enhance the infectivity of baculovirus[25] and retrovirus,[26] but these modifications did not solve the potential virus-related problems (i.e., disturbance of patient's chromosome, and unexpected immunological responses). Our results strongly suggested that BNCs could endow PPX with high transfection efficiency specific to human hepatic cells. Because BNCs attach to and enter into human hepatic cells according to the early infection mechanism of HBV,[8] the BNC–PPX complexes would be incorporated by human hepatic cells in a similar manner. This hypothesis is supported by the excellent transfection efficiency of BNC–PPX complexes of weak positive charge (Fig. 3B). In summary, BNC–PPX complexes would enter into the human hepatic cells specifically via receptor-mediated endocytosis, followed by escape from late endosomes to the cytoplasm presumably induced by the fusogenic activity of BNCs and the proton sponge effect of PEI (Fig. 7).

4. Conclusions

PPX was shown to form stable complexes with BNCs spontaneously, presumably by electrostatic interactions. The BNC–PPX complexes showed excellent transfection efficiency specific to human hepatic cells, presumably due to human liver-specific binding property of BNC, membrane fusogenic activity of BNC, and proton sponge effect of PPX. By combining BNC with modified bio-recognition molecules (e.g., antibodies,[9] lectins,[10] cytokines[7]), the complexes may be retargeted to cells and tissues of interest. Furthermore, since BNC–PPX complexes possess favorable properties for in vivo use, the complexes would be more suitable as an

in vivo pinpoint GDS carrier if cationic polymers of lower cytotoxicity than PEI were available.

Acknowledgements

This work was supported in part by the Naito Foundation (to S.K.), the Canon Foundation (K09-00051, to S.K.), KAKENHI (Grant-in-Aid for Scientific Research (A) (21240052, to S.K.), Grant-in-Aid for Young Scientists (B) (23710143, to M.I.)), and the Program for Promotion of Basic and Applied Researches for Innovations in Bio-oriented Industry (BRAIN) (to S.K.).

References and notes

1. Yokoyama, M. *J. Artif. Organs* **2005**, *8*, 77.
2. Morille, M.; Passirani, C.; Vonarbourg, A.; Clavreul, A.; Benoit, J.-P. *Biomaterials* **2008**, *29*, 3477.
3. Gao, X.; Kim, K.-S.; Liu, D. *AAPS J.* **2007**, *9*, 92.
4. Kaneda, Y.; Iwai, K.; Uchida, T. *Science* **1989**, *243*, 375.
5. Almeida, J. D.; Edwards, D. C.; Brand, C. M.; Heath, T. D. *Lancet* **1975**, *306*, 899.
6. Kuroda, S.; Otaka, S.; Miyazaki, T.; Nakao, M.; Fujisawa, Y. *J. Biol. Chem.* **1992**, *267*, 1953.
7. Yamada, T.; Iwasaki, Y.; Tada, H.; Iwabuki, H.; Chuah, M. K. L.; VandenDriessche, T.; Fukuda, H.; Kondo, A.; Ueda, M.; Seno, M.; Tanizawa, K.; Kuroda, S. *Nat. Biotechnol.* **2003**, *21*, 885.
8. Yamada, M.; Oeda, A.; Jung, J.; Iijima, M.; Yoshimoto, N.; Niimi, T.; Jeong, S.-Y.; Choi, E. K.; Tanizawa, K.; Kuroda, S. *J. Control. Release* **2011**.
9. Tsutsui, Y.; Tomizawa, K.; Nagita, M.; Michiue, H.; Nishiki, T.-ichi; Ohmori, I.; Seno, M.; Matsui, H. *J. Control. Release* **2007**, *122*, 159.
10. Kasuya, T.; Jung, J.; Kadoya, H.; Matsuzaki, T.; Tatematsu, K.; Okajima, T.; Miyoshi, E.; Tanizawa, K.; Kuroda, S. *Hum. Gene Ther.* **2008**, *19*, 887.
11. Jung, J.; Matsuzaki, T.; Tatematsu, K.; Okajima, T.; Tanizawa, K.; Kuroda, S. *J. Control. Release* **2008**, *126*, 255.
12. Merdan, T.; Kopecek, J.; Kissel, T. *Adv. Drug Delivery Rev.* **2002**, *54*, 715.
13. Jung, J.; Iijima, M.; Yoshimoto, N.; Sasaki, M.; Niimi, T.; Tatematsu, K.; Jeong, S.-Y.; Choi, E. K.; Tanizawa, K.; Kuroda, S. *Protein Expr. Purif.* **2011**, *78*, 149.
14. Oku, N.; Tokudome, Y.; Tsukada, H.; Okada, S. *BBA-Biomembranes* **1995**, *1238*, 86.
15. Ogris, M.; Brunner, S.; Schuller, S.; Kircheis, R.; Wagner, E. *Gene Ther.* **1999**, *6*, 595.
16. Bowman, E. J.; Siebers, A.; Altendorf, K. *PNAS* **1988**, *85*, 7972.
17. Rodríguez-Crespo, I.; Núñez, E.; Gómez-Gutiérrez, J.; Yélamos, B.; Albar, J. P.; Peterson, D. L.; Gavilanes, F. *J. Gen. Virol.* **1995**, *76*, 301.
18. Oess, S.; Hildt, E. *Gene Ther.* **2000**, *7*, 750.
19. Neu, M.; Fischer, D.; Kissel, T. *J. Gene Med.* **2005**, *7*, 992.
20. Park, K.; Lee, M.-Y.; Kim, K. S.; Hahn, S. K. *Biomaterials* **2010**, *31*, 5258.
21. Ou, M.; Wang, X.-L.; Xu, R.; Chang, C.-W.; Bull, D. A.; Kim, S. W. *Bioconjug. Chem.* **2008**, *19*, 626.
22. Germershaus, O.; Merdan, T.; Bakowsky, U.; Behe, M.; Kissel, T. *Bioconjug. Chem.* **2006**, *17*, 1190.
23. Suh, W.; Han, S.-O.; Yu, L.; Kim, S. W. *Mol. Ther.* **2002**, *6*, 664.
24. Jiang, G.; Park, K.; Kim, J.; Kim, K. S.; Oh, E. J.; Kang, H.; Han, S.-E.; Oh, Y.-K.; Park, T. G.; Kwang Hahn, S. *Biopolymers* **2008**, *89*, 635.
25. Kim, Y.-K.; Choi, J. Y.; Jiang, H.-L.; Arote, R.; Jere, D.; Cho, M.-H.; Je, Y. H.; Cho, C.-S. *Virology* **2009**, *387*, 89.
26. Ramsey, J. D.; Vu, H. N.; Pack, D. W. *J. Control. Release* **2010**, *144*, 39.